



Trans. Nonferrous Met. Soc. China 34(2024) 3185-3193

Transactions of Nonferrous Metals Society of China

www.tnmsc.cn



Cryogenic springback of 2219-W aluminum alloy sheet through V-shaped bending

Xiao-bo FAN¹, Qi-liang WANG¹, Fang-xing WU¹, Xu-gang WANG²

- 1. School of Mechanical Engineering, Dalian University of Technology, Dalian 116081, China;
- 2. School of Materials Science and Engineering, Harbin Institute of Technology, Harbin 150096, China

Received 28 March 2023; accepted 7 November 2023

Abstract: A V-shaped bending device was established to evaluate the effects of temperature and bending fillet radius on springback behavior of 2219-W aluminum alloy at cryogenic temperatures. The cryogenic springback mechanism was elucidated through mechanical analyses and numerical simulations. The results indicated that the springback angle at cryogenic temperatures was greater than that at room temperature. The springback angle increased further as the temperature returned to ambient conditions, attributed to the combined effects of the "dual enhancement effect" and thermal expansion. Notably, a critical fillet radius made the springback angle zero for 90° V-shaped bending. The critical fillet radius at cryogenic temperatures was smaller than that at room temperature, owing to the influence of temperature variations on the bending moment ratio between the forward bending section at the fillet and the reverse bending section of the straight arm.

Key words: 2219-W aluminum alloy; cryogenic forming; V-shape bending; springback; critical fillet radius

1 Introduction

Recently, various advanced cold- and hotforming methods have been developed to address the limitations of wrinkling and splitting defects generated during the forming process [1–4]. However, the fabrication of large, integral, thin-walled aluminum alloy components remains problematic when conventional cold, hot, or warm forming processes are utilized [5]. Recently, innovative technology for cryogenic temperature formation has been developed based on the novel phenomenon of the "dual enhancement effect" of aluminum alloys. This technology is aimed at the integral formation of thin-walled aluminum alloy shells to overcome the problems of wrinkling and splitting in cold and hot forming processes [5–7]. Cryogenic temperatures improve the mechanical

properties of aluminum alloys and address the problem of conventional aluminum alloy surface roughness [8]. Cryogenic forming is an emerging process method; most studies on this method have been primarily focused on analyzing the microstructures. However, the application of parts requires formability while ensuring that the size of the parts meets the design requirements. As a critical issue affecting the size of parts, relevant research on cryogenic springback remains limited.

As a frequent problem in sheet metal forming, springback has been extensively studied [9–14]. Many experimental methods have been employed in springback research, including U-profile bending, L-die bending, air bending, and V-shaped bending [15–20]. V-shaped bending is widely utilized for the springback analysis of various materials owing to its significant springback and simpler operation. PARK et al [21] evaluated the effect of

Mn content and austenitizing temperature on the springback of medium-manganese steel employing a V-bending test. The results revealed that, when the forming temperature is 300-500 °C, the proportion of martensitic transformation increased with Mn content, resulting in large springback of medium- manganese steel. NURI and VEDAT [22] conducted experiments employing V-bending test at room temperature (RT) to clarify the formability of high-strength multiphase CP800 sheets. Three punch radii and two holding time were adopted in these experiments. The results indicated that the springback of the CP800 sheets increased with an increase in the punch radius, whereas the effect of the holding time on the springback of the material was limited. YANG et al [23] studied the springback of a TC4 titanium alloy subjected to V-bending hot stamping. The experimental results revealed that the TC4 titanium alloy broke at RT, exhibited good formability at 750-900 °C, but had serious springback. The factors affecting springback primarily include the material thickness, punch radius, bending angle, holding time, and temperature. **THIPPRAKMAS** forming PHANITWONG [24] studied process parameters such as material thickness, V-bend angle, and punch radius, employing a numerical model and Taguchi technology. The results indicated that the sheet thickness had significantly impacted the springback. In an experiment with a fixed material thickness, the springback can only be controlled by other factors. NURI et al [25] conducted V-shaped bending tests with different die angles and punch radius to study the effect of die parameters on the springback behavior of MART 1400 steel. The results indicated that an increase in the die angle and punch radius increased the springback. MA et al [26] studied the effect of initial temperature of a 6061 aluminum alloy sheet on the forming process. The results revealed that springback angle decreased with increasing initial temperature of the sheet, and the beneficial initial blank temperature for 6016 aluminum alloy to reduce the springback was 400-500 °C. ZONG et al [27] conducted V-bending tests of a Ti-6Al-4V alloy sheet from RT to 850 °C and utilized four punch radii. The experimental results revealed that the impact of the punch radius on springback differed at different temperatures. Mold size and forming temperature are crucial for springback control.

In this study, cryogenic temperature V-shaped bending device was established to achieve the V-shaped bending from 25 to -196 °C to reveal the effects of temperature and punch radius on bending and springback. The springback mechanism of V-shaped bending was elucidated based on numerical simulation and mechanical analysis.

2 Experimental

2.1 Material

A 2 mm-thick annealed 2219 aluminum alloy sheet was used in this study. The quenched state (W-temper), which has the best formability, is widely used in cryogenic forming. Therefore, the W-temper 2219 aluminum alloy was selected as the research object. The specimens were heated to 535 °C for 90 min in a resistance heating furnace with a temperature control accuracy of ±2 °C and then rapidly quenched into water. The specimens were frozen in liquid nitrogen (LN₂) after heat treatment to avoid natural aging. The axial mechanical properties of the material at different temperatures were obtained via uniaxial tensile tests with a crosshead speed of 4.2 mm/min. The gauge section was 70.0 and 10.0 mm in length and width, respectively. Figure 1 shows the true stress-strain relationships at different temperatures. Table 1 presents the primary mechanical properties at different temperatures.

2.2 Experimental methods

A cryogenic bending device capable of achieving temperatures from 25 °C to -196 °C was

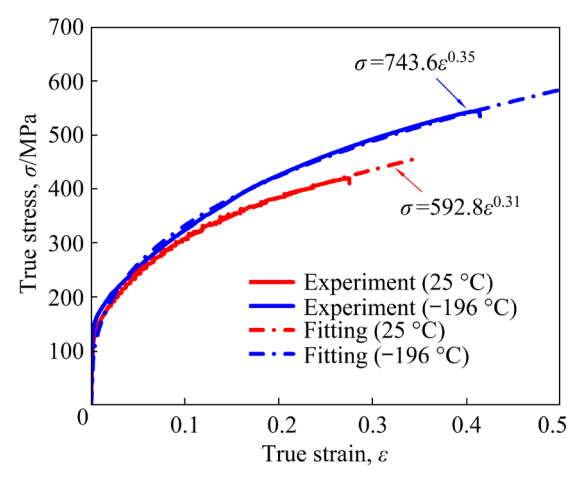


Fig. 1 True stress-strain curves of 2219-W aluminum alloy sheet at different temperatures

Table 1 Main mechanical properties of 2219-W aluminum alloy sheet at different temperatures

Temperature/ °C	Yield strength/ MPa	Ultimate tensile strength/MPa	Elastic modulus/MPa
25	129.6	321.3	70000
-196	158.0	366.4	70000

established to facilitate cryogenic bending. The device consisted of a 30 t tensile tester, temperature control box, and bending dies, as shown in Fig. 2. The bending experiment at −196 °C was conducted by soaking in LN₂. The dies and specimens were flooded with LN₂ before the experiment. When the boiling stopped at the LN₂ level and the real-time tensile force of the drawing machine was stable, the mold temperature reached a constant temperature of -196 °C. The specimen was designed as a strip with a length and width of 120 mm and 50 mm, respectively. The opening angle of the female die was 90°, with the gap between the male and female dies set to be 2 mm. Bending was performed at quasi-static speed, and the targeted bending angle of the final specimen was 90°.

For cryogenic forming, LN₂ with a temperature of –196 °C is commonly used. Therefore, this study was focused on a temperature of –196 °C to study the law of springback at cryogenic temperature. RT bending was selected for comparison. Moreover, the punch radius is an important factor that affects springback. Therefore, five different punch radii were designed for the cryogenic bending experiments. The bending strain for all conditions was pre-

calculated and compared with the ultimate strain to ensure no fracture defects. The detailed research scheme is presented in Table 2. To obtain the springback law of the V-shaped specimen at cryogenic temperatures, the profile of the test specimen was immediately recorded, and the angle after cryogenic temperature bending was measured. As most specimens obtained through cryogenic temperature forming are used at RT, the temperature recovery of the specimens can affect the bending angle. After the bending specimens recovered to RT, the profile was recorded and the angle was remeasured. The angle obtained by measuring the V-shaped specimen was the bending angle, and the difference between the bending angle and opening angles of the female die was the springback angle of the V-shaped specimen. Three experiments were conducted for each condition, with the average value calculated for analysis.

2.3 Numerical model

The numerical modeling was performed by employing Abaqus 6.14, where a dynamic explicit solver was adopted, as shown in Fig. 3. The sheet was defined as a deformable body meshed using C3D8R elements. The element size was 0.5 mm, and four layers were assigned in the thickness direction. The number of elements was 96000 approximately. The punch and die were modeled as discrete rigid bodies with a mesh size of 1 mm. Cooling shrinkage deformation of the mold was not considered in the model.

The contact between the sheet and bending tools was modeled employing a surface-to-surface

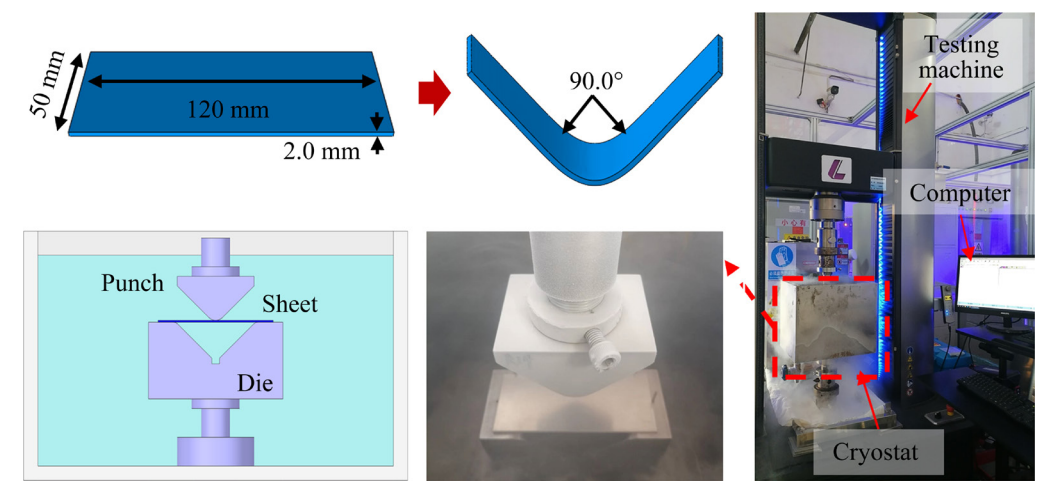


Fig. 2 Cryogenic V-shaped bending device

Table 2 Experimental scheme

Heat	Test temperature/	Punch
treatment state	°C	radius/mm
Quenched (W-temper)	25	2, 4, 6, 10, 14
Quenched (W-temper)	-196	2, 4, 6, 10, 14

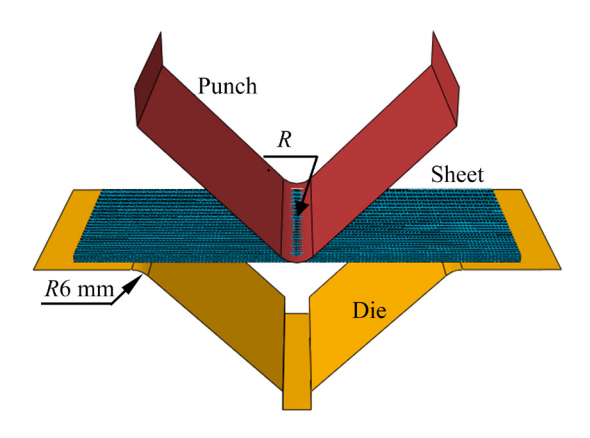


Fig. 3 Numerical model for V-shape bending at cryogenic temperature

approach based on the penalty-function method. By comparing the similarity degree of the force—displacement curves obtained from the simulation with different friction coefficients (μ) and the experiment, the same friction coefficient of 0.3 between the sheet and tools was adopted, as shown in Fig. 4. The loading process was simulated by using ABAQUS/Explicit, whereas springback was simulated by using ABAQUS/Standard. The results from the last step of ABAQUS/Explicit simulation were imported into ABAQUS/ Standard simulation to serve as a predefined state for the springback simulation. The node coordinates of the sidewall of

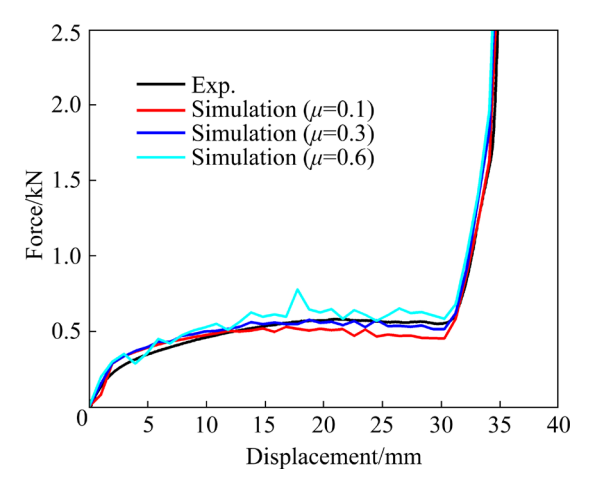


Fig. 4 Comparison of force—displacement curves obtained from experiments and simulations with different friction coefficients

the specimen were extracted from the simulation results to measure the springback angle. During the simulation, the movement of the female die was restricted in all directions, only the longitudinal movement of the male die was allowed, and the sheet was placed freely on the female die. The plastic parameters employed in the simulation were determined by using the Swift in Fig. 1.

3 Results and discussion

3.1 Effects of temperature and punch radius on springback

A cryogenic V-shaped bending experiment with five different punch radii was conducted to evaluate the effect of the punch radius on the springback of the V-shaped specimens. The contour curve of the specimen after returning to RT is shown in Fig. 5. When the punch radius was 2 mm, the bending angle measured 87.9° and the springback angle was -2.1°. As the punch radius increased to 6 mm, the bending angle measured 89.9° and the springback angle decreased to -0.1° . As the punch radius increased, the bending angle gradually increased, and the springback angle transitioned from negative to positive. Notably, the critical punch radii of 6 mm negative springback occurred when the punch radius was less than 6 mm. Conversely, when the punch radius was greater than 6 mm, positive springback was observed.

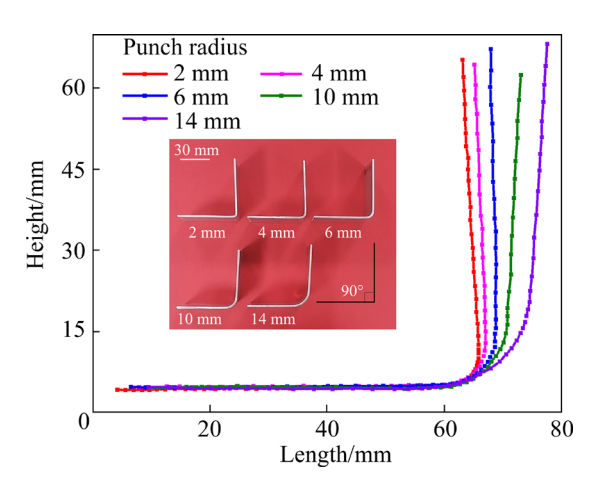


Fig. 5 Profiles with different punch radii

To study the effect of temperature on springback, two typical punch radii, 4 and 14 mm, were selected for V-shaped bending experiments at RT and -196 °C. The profiles of the V-shaped samples at corresponding temperatures are shown

in Fig. 6. When the punch radius was 4 mm, the bending angles of the specimens obtained at RT and cryogenic temperature were 87.7° and 88.6° respectively, and the springback angles were -2.3° and -1.4° respectively. When the punch radius was 14 mm, the bending angles of the test specimens obtained at RT and cryogenic temperature were 92.1° and 93.8°, respectively, and the springback angles were 2.1° and 3.8°, respectively. The bending angle of the specimens formed at -196 °C is larger than that of the specimens formed at RT with the same punch radius. The cryogenic temperature weakened the negative springback of the V-shaped specimens and increased their positive springback.

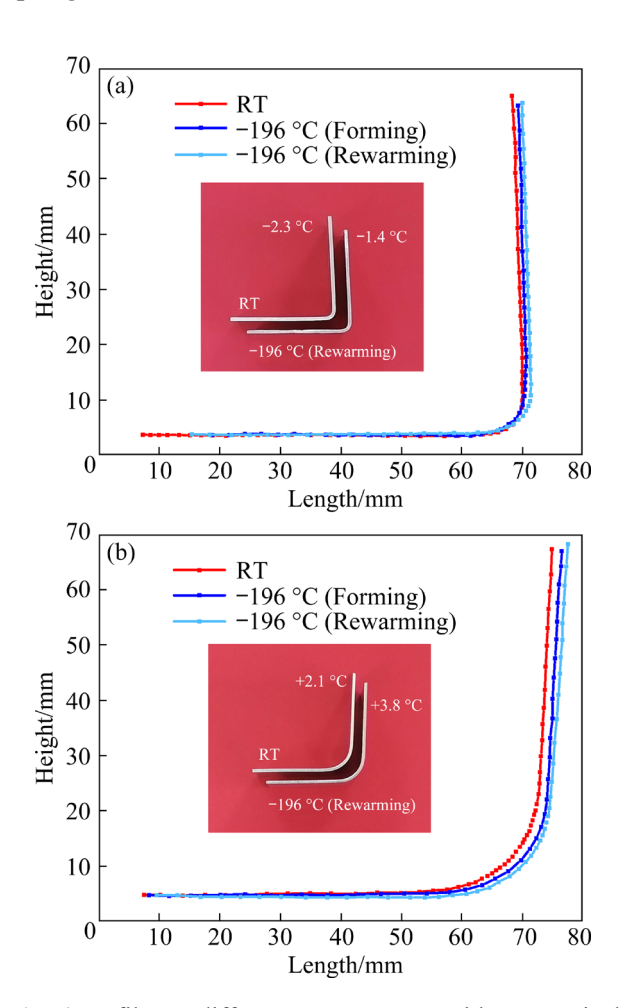


Fig. 6 Profiles at different temperatures with two typical punch radii: (a) 4 mm; (b) 14 mm

Figure 7 shows the springback behavior of the V-shaped specimens at various forming temperatures and punch radii, indicating that a smaller punch radius results in negative springback, whereas a larger punch radius results in positive springback. As the punch radius increased, the

springback angle gradually transitioned from negative to positive. There is a critical value or punch radius that makes the springback angle zero. The critical value of punch radius increases with an increase in temperature. For example, the critical springback value of V-shaped specimens is 6 mm at -196 °C, whereas it is 10 mm at RT. After forming and springback at cryogenic temperatures, the bending angle of the V-shaped specimens increased after recovering to RT, leading to an average increase of 0.5° in the springback angle. Hence, if the selected punch radius is less than 6 mm when the experiment is conducted at cryogenic temperature, it is necessary to control the negative springback. Conversely, if the selected punch radius is greater than 6 mm, it is necessary to control the positive springback. In the experiment conducted at RT, the positive and negative springbacks are controlled using 10 mm of punch radius as the dividing point.

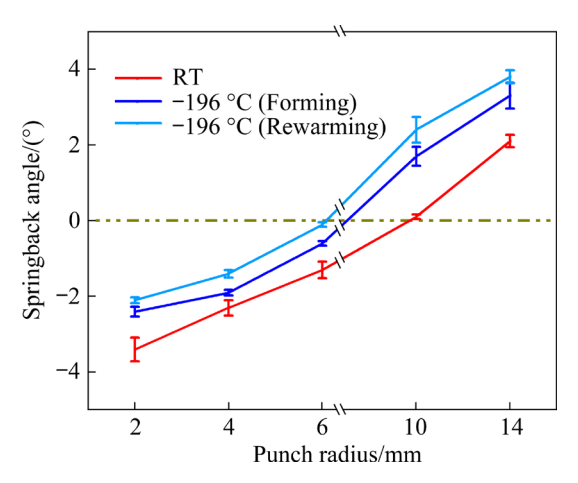


Fig. 7 Springback angle varying with punch radius at different temperatures

3.2 Deformation and springback behavior

3.2.1 V-shaped bending deformation behavior

The V-shaped bending can be divided into three stages: three-point, partial, and full-surface contact [27]. Throughout the bending process, the outer and inner layers of the bending zone are influenced by tensile and compressive stresses, respectively. Figure 8 shows the principal stress distribution at the V-shaped bending loading stage. In the initial stage (Fig. 8(a)), the top of the punch contacted the sheet and pushed the center of the sheet downward. The two ends of the sheet were warped. At this time, the sheet contacted both the punch fillet and the two shoulder fillets of the

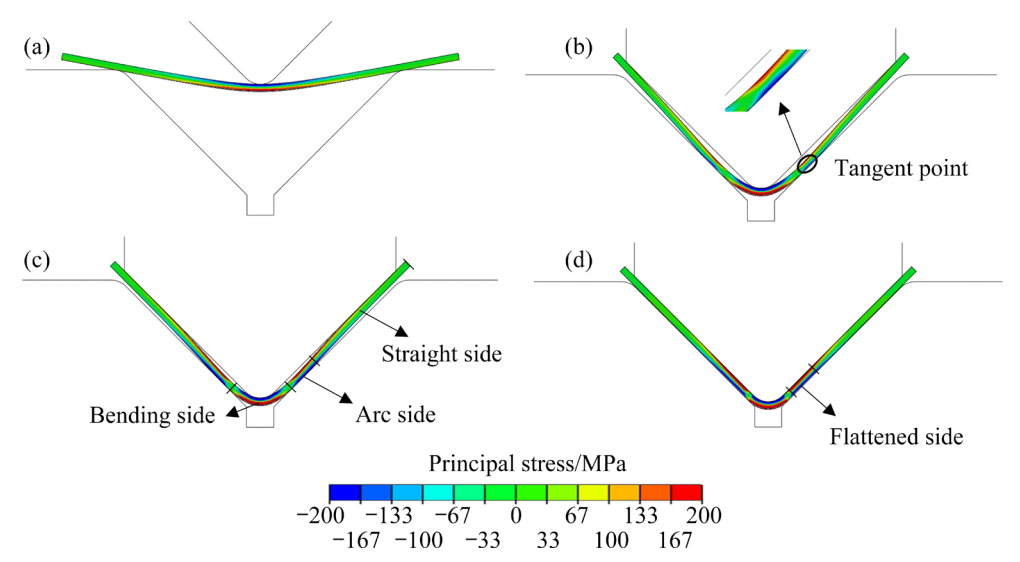


Fig. 8 Distribution of principal stress in V-shaped bending loading process: (a) Three-point bending stage; (b) Initial stage of partial surface contact; (c) End stage of partial surface contact; (d) Full surface contact stage

female die. In the contact area with the punch radius, the stress distribution in the sheet resulted in external tension and internal pressure. In the subsequent stage (Fig. 8(b)), the sheet slid into a concave die. Some areas on the side of the V-shaped specimen contacted the die wall, and the transition area between the straight-wall section and bending zone formed a small arc. The contact part between the side of the V-shaped specimen and the die wall produced a stress distribution of the external pressure and internal tension opposite to the bending zone. As the punch descended further (Fig. 8(c)), the contact area between the side of the V-shaped specimen and the die wall decreased, expanding the arc region. Consequently, the areas of external compressive stress and internal tensile stress increased. After loading was completed (Fig. 8(d)), the V-shaped specimen was tightly pressed between the punch and die sidewalls, and the small arc of the transition region became flattened. The specimen achieved a 90° bending angle, and its sidewall underwent a complex stress contact. The bending zone and arc section formed the opposite stress states, resulting in positive and negative springback of the specimen at different punch radii and temperatures.

3.2.2 Effect of punch radius on springback behavior

The influence of the punch radius on springback was analyzed through numerical simulations. A comparison diagram of the principal stress in the test specimens with different punch radii at cryogenic temperatures was obtained, as

shown in Fig. 9. It was evident that, as the punch radius increased gradually, the principal stress distribution area of the bending zone extended from 9.0 to 23.0 mm, whereas the principal stress distribution area of the reverse bending zone reduced from 18.0 to 8.0 mm. An increase in the principal stress distribution area in the bending zone led to a higher outward tension angle of the specimen after unloading, whereas a decrease in the principal stress distribution area in the reverse bending zone resulted in a reduced inward tension angle of the specimen after unloading. When the punch radius reached 6 mm, the influences of the principal stress in the bending zone and that in the reverse bending zone on the V-shaped specimen were offset, resulting in the test specimen exhibiting no significant springback. As the punch radius increased, the influence of the principal stress in the bending zone became greater than that in the reverse bending zone, and the test specimen produced a positive springback. The punch radius affected the final springback angle of the test specimen by influencing the stress distribution in its bending and reverse bending zones of the test specimen.

3.2.3 Effect of temperature on springback behavior

During bending, the outer and inner layers of the bending zone are influenced by tensile and compressive stresses, respectively. Figure 10 shows the stress distribution on the cross-section of the sheet metal during bending. In the inner and outer layers, the tangential stress was far larger than the

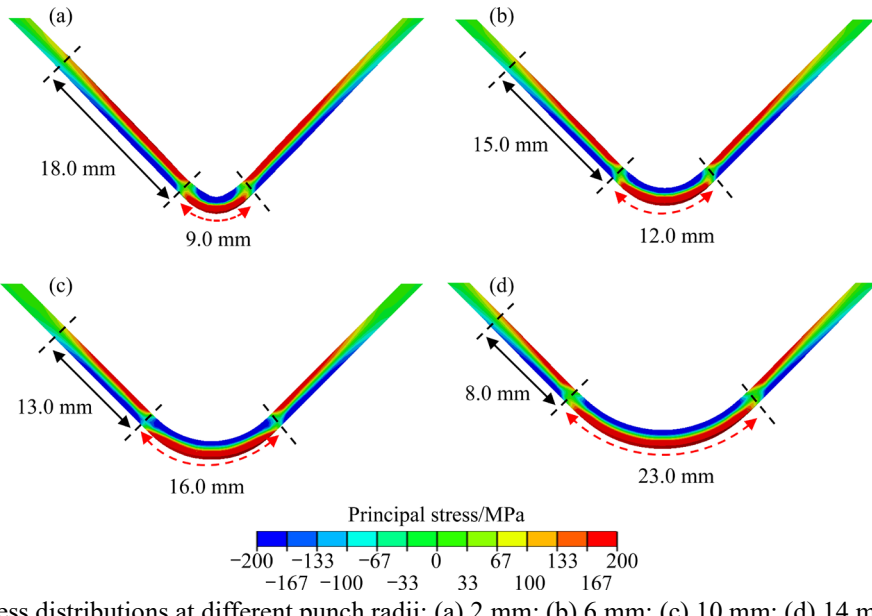


Fig. 9 Principal stress distributions at different punch radii: (a) 2 mm; (b) 6 mm; (c) 10 mm; (d) 14 mm

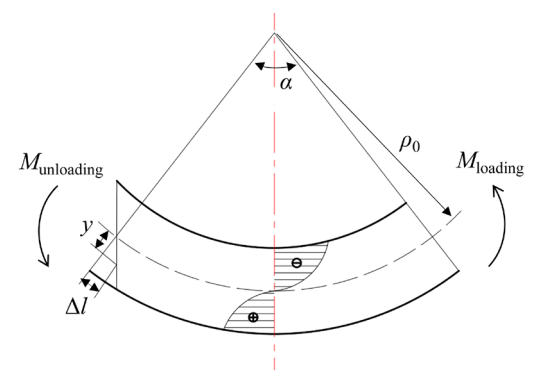


Fig. 10 Stress distribution of sheet metal after bending

thickness and transverse stresses because the material flowed mainly along the tangential direction. In the calculations, only the case of a large punch radius was considered. The springback angle of the V-shaped specimen was dominated by the bending section and was positive. The thickness stress and transverse stress were ignored. The elastic stress was assumed to be symmetrically distributed in the inner and outer layers. According to the bending moment, the springback angle ($\Delta \alpha$) is expressed as follows [28]:

$$\Delta \alpha = \frac{12\rho_0 \alpha M_{\text{unloading}}}{Ebt^3} \tag{1}$$

where b denotes the width of the specimen, t is the thickness of the specimen, ρ_0 is the radius of the neutral layer, $M_{\text{unloading}}$ is the bending moment before unloading, and E is the elastic modulus.

Notably, the springback angle is proportional to the bending moment before unloading, but inversely proportional to the elastic modulus, sheet width and sheet thickness.

Considering $M_{\text{unloading}} = M_{\text{loading}}$, then

$$\Delta \alpha = \frac{12\rho_0 \alpha}{Ebt^3} \int_0^{\frac{h}{2}} \sigma y b dy = \frac{24\rho_0 \alpha}{Ebt^3} \int_0^{\frac{h}{2}} K \left(\frac{y}{\rho_0}\right)^n y b dy = \frac{3Kt^{(n-1)} \alpha}{(n+2)2^{(n-1)}\rho_0^{n-1}E}$$
(2)

where y is the distance from any layer to a neutral layer on the bending side, K is the strengthening coefficient, and *n* is the hardening index.

Equation (2) implies that the temperature influences the springback angle of a V-shaped specimen by affecting the strengthening coefficient, hardening index, and elastic modulus. However, the elastic modulus at different temperatures does not exhibit much difference for the same material. Therefore, the influence of elastic modulus was not considered, and elastic modulus was regarded as a constant.

Strengthening coefficient and hardening index for most aluminum alloys in forming state are in the ranges of 300-800 and 0.2-0.5, respectively. For a sheet with a thickness of 2 mm, the punch radius of 10 mm was taken as an example to calculate the springback angle within this range, and a scatter diagram of the springback angle was obtained to change with the strengthening coefficient and hardening index, as shown in Fig. 11. When n was

held constant, increasing K led to an increase in the springback angle. When K was constant, increasing n led to a decrease in the springback angle. Smaller K values and larger n values led to lower springback angles. As shown in Fig. 1, the K and K values for the 2219-W aluminum alloy at $-196\,^{\circ}$ C were 743.6 and 0.35, respectively, whereas at RT, they were 592.8 and 0.31, respectively. Comprehensively considering the two variables, the springback angle at cryogenic temperatures was greater.

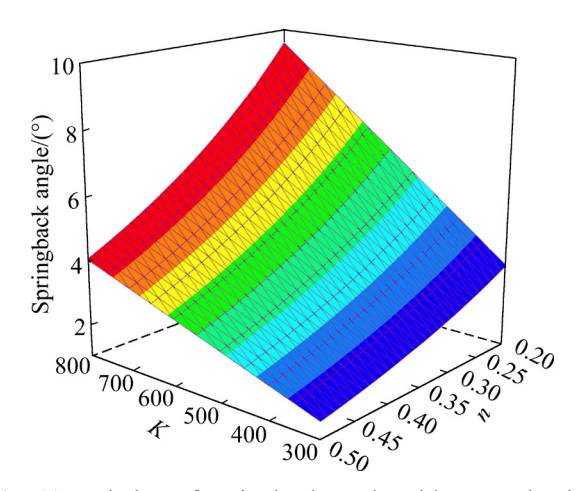


Fig. 11 Variation of springback angle with strengthening coefficient (K) and hardening index (n)

4 Conclusions

- (1) The cryogenic temperature weakened the negative springback and increased the positive springback. The springback angle at cryogenic temperatures was consistently larger than that observed at RT at the same punch radius. Further, the bending angle increased while recovering from -196 °C to RT, leading to an average increase of 0.5° in the springback angle.
- (2) The bending angle increased with the punch radius, and the springback angle changed from negative to positive. The positive and negative springback of the V-shaped specimens was attributed to the opposing stress states in the bending and reverse bending zones.
- (3) Temperature has a significant effect on the critical radius. At cryogenic temperatures, the critical radius was 6 mm, whereas at RT, it was 10 mm. The discovery of the cryogenic springback law is of great significance in fillet design because it provides important guidance for springback control in actual cryogenic forming.

CRediT authorship contribution statement

Xiao-bo FAN: Conceptualization, Methodology, Writing – Review & editing, Supervision, Resources; Qi-liang WANG: Conceptualization, Methodology, Software, Investigation, Formal analysis, Writing – Original draft; Fang-xing WU: Writing – Review & editing, Supervision; Xu-gang WANG: Writing – Review & editing, Supervision.

Declaration of competing interest

The authors declare that they have no known competing financial interests or personal relationships that could have appeared to influence the work reported in this paper.

Acknowledgments

The authors are grateful for the financial supports from the National Key Research and Development Program of China (No. 2019YFA0708804).

References

- [1] WANG Peng-yi, WAN Ge-hui, JIN Jia-geng, WANG Yu-cong, XIANG Nan, ZHAO Xiao-kai, ZHAO Xue-ni, YUAN Bin-xian, WANG Zong-jin. Subregional flexible-die control in magnetorheological pressure forming [J]. Journal of Materials Processing Technology, 2022, 307: 117698.
- [2] JIAO Zhi-hui, LANG Li-hui, ZHAO Xiang-ni. 5A06-O aluminium-magnesium alloy sheet warm hydroforming and optimization of process parameters [J]. Transactions of Nonferrous Metals Society of China, 2021, 31(10): 2939-2948.
- [3] AL-HAMMADI R A, ZHANG Rui, CUI Chuan-yong, ZHOU Zi-jian, ZHOU Yi-zhou. Superplastic behavior of a Ni–Co-base superalloy with high γ'-phase content [J]. Materials Letters, 2023, 348: 134683.
- [4] CHEN Yi-zhe, ZHAO Shi-long, WANG Hui, LI Jun, HUA Lin. Theoretical analysis and verification on plastic deformation behavior of rocket nozzle using a novel tube upsetting-bulging method [J]. Materials, 2023, 16(4): 1680.
- [5] FAN Xiao-bo, CHEN Xian-shuo, YUAN Shi-jian. Novel forming process for aluminum alloy thin shells at ultra-low temperature gradient [J]. International Journal of Machine Tools and Manufacture, 2023, 185: 103992.
- [6] FAN Xiao-bo, YUAN Shi-jian. Innovation for forming aluminum alloy thin shells at ultra-low temperature by the dual enhancement effect [J]. International Journal of Extreme Manufacturing, 2022, 4: 103–107.
- [7] CHEN Xian-shuo, FAN Xiao-bo, XU Ai-jun, YI Zhou-xun, YUAN Shi-jian. Formability enhancement and deformation mechanism of 2195 Al–Li alloy sheet in cryogenic forming [J]. Materials Characterization, 2023, 196: 112577.
- [8] PADMINI B V, SAMPATHKUMARAN P, SEETHARAMU S, NAVEEN G J, NIRANJAN H B. Investigation on the wear behaviour of aluminium alloys at cryogenic temperature and subjected to cryo-treatment [J]. IOP Conference Series: Materials Science and Engineering, 2019, 502: 012191.

- [9] ZANG S L, LIANG J, GUO C. A constitutive model for spring-back prediction in which the change of young's modulus with plastic deformation is considered [J]. International Journal of Machine Tools and Manufacture, 2007, 47: 1791-1797.
- [10] WANG Kai, ZHAN Li-hua, YANG You-liang, MA Zi-yao, LI Xi-cai, LIU Jian. Constitutive modeling and springback prediction of stress relaxation age forming of pre-deformed 2219 aluminum alloy [J]. Transactions of Nonferrous Metals Society of China, 2019, 29(6): 1152-1160.
- [11] WANG J, VERMA S, ALEXANDER R, GAUC J. Spring-back control of sheet metal air bending process [J]. Journal of Manufacturing Processes, 2008, 10: 21-27.
- [12] HAN Fei, MO Jan-hua, QI Hong-wei, LONG Rui-fen, CUI Xiao-hui, LI Zhong-wei. Springback predication for incremental sheet forming based on FEM-PSONN technology [J]. Transactions of Nonferrous Metals Society of China, 2013, 23: 1061-1071.
- [13] KIM H S, KOC M. Numerical investigations on springback characteristics of aluminum sheet metal alloys in warm forming conditions [J]. Journal of Materials Processing Tech, 2008, 204: 370-383.
- [14] PANTHI S K, RAMAKRISHNAN N. Semi analytical modeling of springback in arc bending and effect of forming load [J]. Transactions of Nonferrous Metals Society of China 2011, 21(10): 2276-2284.
- [15] JAMLI M R, ARIFFIN A K, WAHAB D A. Incorporating feedforward neural network within finite element analysis for L-bending springback prediction [J]. Expert Systems with Applications, 2015, 42: 2604-2614.
- [16] VALINEZHAD M, ETEMADI E, HASHEMI R, VALINEZHAD M. Experimental and FE analysis on spring-back of copper/aluminum layers sheet for a L-die bending process [J]. Materials Research Express, 2019, 6: 1165h4.
- [17] HE Wei-lin, MENG Bao, SONG Bing-yi, WAN Min. Grain size effect on cyclic deformation behavior and springback prediction of Ni-based superalloy foil [J]. Transactions of Nonferrous Metals Society of China, 2022, 32(4): 1188-1204.
- [18] VORKOV V, AERENCE R, VANDEPITTE D, DUFLOU J R. Two regression approaches for prediction of large radius air bending [J]. International Journal of Material Forming,

[19] QUADFASEL A, LOHMAR J, HIRT G. Investigations on

2019. 12(3): 379-390.

- springback in high manganese twip-steels using U-profile draw bending [J]. Procedia Engineering, 2017, 207: 1582-1587.
- [20] HANG Gang-sheng, WANG Yan-xia, WANG Li-fei, HAN Ting-zhuang, PAN Fu-sheng. Effects of grain size on shift of neutral layer of AZ31 magnesium ally under warm condition [J]. Transactions of Nonferrous Metals Society of China, 2022, 20(3): 1481-1494.
- [21] PARK A R, NAM J H, KIM M, JANG I S, LEE Y K. Evaluations of tensile properties as a function of austenitizing temperature and springback by V-bending testing in medium-Mn steels [J]. Materials Science & Engineering A, 2020, 787: 139534.
- [22] NURI S, VEDAT T. Experimental and numerical investigation of the springback behaviour of CP800 sheet after the V-bending process [J]. Ironmaking & Steelmaking, 2021, 48: 811-818.
- [23] YANG Xiao-ming, DANG Li-ming, WANG Yao-qi, Zhou Jing, WANG Bao-yu. Springback prediction of TC4 titanium alloy V-bending under hot stamping condition [J]. Journal of Central South University, 2020, 27: 2578-2591.
- [24] THIPPRAKMAS S, PHANITWONG W. Process parameter design of spring-back and spring-go in V-bending process using Taguchi technique [J]. Materials & Design, 2011, 32: 4430-4436.
- [25] NURI Ş, TOLGAHAN C, ÖMER S. Experimental, analytical and parametric evaluation of the springback behavior of MART1400 sheets [J]. Journal of the Brazilian Society of Mechanical Sciences and Engineering, 2022, 44:
- [26] MA Wei-ping, WANG Bao-yu, XIAO Wen-chao. Springback analysis of 6016 aluminum alloy sheet in hot V-shape stamping [J]. Journal of Central South University, 2019, 26: 524-535.
- [27] ZONG Ying-ying, LIU Po, GUO Bin, SHAN De-bin. Springback evaluation in hot V-bending of Ti-6Al-4V alloy sheets [J]. The International Journal of Advanced Manufacturing Technology, 2015, 76: 577-585.
- [28] XIONG Zhi-qing, LIN Zhao-rong. A study of the hot sizing and high temperature mechanical behavior of titanium sheet [J]. CIRP Ann Manuf Technol, 1983, 32: 161-165.

2219 固溶态铝合金超低温 V 形弯曲回弹

凡晓波1, 王启梁1, 邬方兴1, 王旭刚2

- 1. 大连理工大学 机械工程学院, 大连 116081;
- 2. 哈尔滨工业大学 材料科学与工程学院,哈尔滨 150096

摘 要:通过建立超低温 V 形压弯装置,确定温度和凸模半径对 2219 固溶态铝合金超低温回弹的影响,并进行 力学分析和数值模拟揭示超低温回弹机制。结果表明,超低温回弹角略大于常温,在恢复至常温的过程中,回弹 角进一步增大,这是由于"双增效应"和热膨胀的影响。90°V形弯曲存在一个回弹角为零的临界圆角半径,且 超低温临界圆角半径小于常温,这是由于圆角弯曲段和直臂反弯曲段的正负弯矩比受到超低温耦合的影响。

关键词: 2219-W 铝合金; 超低温成形; V 形弯曲; 回弹; 临界圆角半径